

1 *Article*

# 2 **Spatial Dependence Modeling of Wind Resource under** 3 **Uncertainty Using C-Vine Copulas and Its Impact on** 4 **Solar-Wind Energy Co-Generation**

5 **Apurva Narayan**<sup>1, \*</sup>, **Kumaraswamy Ponnambalam**<sup>1</sup> and **Sheree A. Pagsuyoin**<sup>2</sup>

6 <sup>1</sup> University of Waterloo, Ontario, Canada N2L 3G1; {a22naray, ponnu}@uwaterloo.ca

7 <sup>2</sup> University of Massachusetts Lowell, Massachusetts, USA 01854; Sheree\_Pagsuyoin@uml.edu

8 \* Correspondence: a22naray@uwaterloo.ca, Tel.: +1-519-888-4567 x31450

9 **Abstract:** Investments in wind and solar power are driven by the aim to maximize the utilization of  
10 renewable energy (RE). This results in an increased concentration of wind farms at locations with higher  
11 average wind speeds and of solar panel installations at sites with higher average solar insolation. This is  
12 unfavourable for energy suppliers and for the overall economy when large power output fluctuations occur.  
13 Thus, when evaluating investment options for spatially distributed RE systems, it is necessary to model  
14 resource fluctuations and power output correlations between locations. In this paper, we propose a  
15 methodology for analyzing the spatial dependence, accurate modeling, and forecasting of wind power  
16 systems with special consideration to spatial dispersion of installation sites. We combine vine-copulas with  
17 the Kumaraswamy distribution to improve accuracy in forecasting wind power from spatially dispersed  
18 wind turbines and to model solar power generated at each location. We then integrate these methods to  
19 formulate an optimization model for allocating wind turbines and solar panels spatially, with an end goal  
20 of maximizing overall power generation while minimizing the variability in power output. A case study of  
21 wind and solar power systems in Central Ontario, Canada is also presented.

22 **Keywords:** renewable energy; wind and solar power; Kumaraswamy distribution; C-Vine copula

## 24 **1. Introduction**

25 Wind power is one of the world's largest and most accessible high intensity renewable energy resource,  
26 with solar power fast becoming a widely implemented renewable resource [1]. Globally, there are  
27 increasing efforts to tap more into these renewable energy sources; however, their intermittent availability  
28 presents one barrier for the renewable energy-based systems to entirely meet energy demands [2]. Wind  
29 fluctuations can be abrupt and significant, causing problems with the ability to generate steady energy  
30 outputs. Also, due to the stochastic nature of wind, it is difficult to accurately forecast wind power  
31 generation by considering only temporal wind behavior when other factors such as wind farm topology and  
32 turbine characteristics are equally important [3]. On the other hand, while the availability of solar energy is  
33 relatively constant, solar power output exhibits high sensitivity to slight changes in solar insolation [4].

34  
35 Another challenge associated with renewable energy systems is their integration into the main power  
36 grid. Renewable energy installations can be geographically sparsely distributed despite being part of the  
37 same power grid, leading to sub-optimal power transactions within the grid [5]. Decisions on where to place

38 these installations are often based on the availability of wind and solar resources in order to maximize  
39 perceived power outputs [6]. This leads to localized concentrations of installations in areas of high wind or  
40 solar availability, which can become highly unfavourable for energy suppliers due to increased power  
41 fluctuations and overall system instability [6].

42

43 Previous researchers have examined the possibility of smoothing fluctuations in wind power  
44 generation through employing geographically dispersed systems, or by interconnecting existing dispersed  
45 systems [7, 8]. For example, system reliability has been found to increase with turbine size in wind farms  
46 [9], while interconnection has been shown to greatly impact the reliability and stability of renewable energy  
47 systems [10].

48

49 In this paper, we propose a methodology for analyzing the spatial dependence, accurate modeling, and  
50 forecasting of wind power generation with special consideration to temporal variations in power output and  
51 spatial dispersion of installation sites. The rest of this paper is organized as follows: Section 2 provides a  
52 brief review of literature related to wind and solar power systems modeling. Section 3 introduces the three  
53 mathematical concepts that serve as the foundations of our proposed methodology: the Kumaraswamy  
54 distribution, the theory of copulas, and vine-copulas. Section 4 discusses our proposed model for the  
55 optimal allocation of renewable energy generation technologies while Section 5 presents a case application  
56 of the proposed methodology. Finally, Section 6 summarizes the findings and intellectual contributions of  
57 this study.

## 58 2. Literature Review

59 Linear correlation coefficients provide general information about the interdependence of wind power  
60 generated at spatially distributed sites [11]; however, they do not uniquely describe the structure of this  
61 dependence [11]. Further, they do not provide actionable information that is helpful to system planners and  
62 operators. For example, linear correlation coefficients are not useful in determining the duration in a year  
63 when the aggregate wind power in a system will be above or below a specified threshold value even when  
64 coupled with data on the marginal distributions of wind power at each installation, as dependence relations  
65 are nonlinear. A potential method for mathematically describing the dependency structure among wind  
66 power systems involves using joint distribution functions [12]. However, multivariate distribution models  
67 are currently not available for such systems, and common joint distributions do not accurately fit wind  
68 power data [12]. A possible workaround suggested by Kroese et al [13] involves decomposing the assumed  
69 correlation matrix using Cholesky decomposition, but this is only applicable if random variables are linearly  
70 correlated.

71

72 It has been demonstrated that wind speeds are characterized by non-normal distributions and non-  
73 linear dependence [6]. This becomes problematic in multivariate analysis; when multivariate data are not  
74 normally distributed, accurate quantiles of the sums of margins cannot be calculated from the sums of  
75 variances and covariances which makes modeling these random variables (wind speeds in our case) more  
76 challenging.

---

77  
78 Goethe and Schnieders [6] modeled the univariate time series of wind speed at several wind farms in  
79 Germany using a seasonal autoregressive moving average (ARMA) model proposed by Benth and Benth  
80 [14]. To model the correlation between multiple wind farm locations, they analyzed the correlation between  
81 the residuals of the various univariate time series and fit copulas to the residuals, thus developing copula-  
82 GARCH (generalized autoregressive conditional heteroskedasticity) models.

83  
84 A more appropriate approach for modeling non-linear, non-normal and more complex dependency  
85 structure in data is by directly using appropriate copulas [6, 15-18]. Copulas are applied widely in finance  
86 [19, 20], and they possess unique characteristics that make them highly attractive in modeling wind power  
87 [18]. Of these characteristics, the most important is the ability of copulas to model the dependence structure  
88 of data independent of the marginal distributions of the participating variables. This feature is very critical  
89 because wind power outputs at different locations are often significant at the grid nodes they are infused  
90 and modeling them using single marginal distribution is not possible. Therefore, finding this dependence  
91 in power outputs independent of marginal distributions is of great advantage for system planners as it allows  
92 modeling wind power generation more accurately.

93  
94 The correlations among wind power generated at different locations are usually estimated from  
95 parameters such as separation distance and averaging period, among others [21, 22, 23]. If only basic  
96 information is available about the locations of wind turbines, an accurate model of the dependency structure  
97 of wind power generated at these locations can be produced using copulas. Consequently, the selection of  
98 an appropriate copula function is very important, as inappropriate selection can lead to unacceptable errors.  
99 Of all copulas, the Gaussian copula is the most commonly used copula due to its computational  
100 convenience; however, its suitability in wind power analysis has not been rigorously investigated. The  
101 standard Gaussian copula has been previously used to model wind power in Europe based on a qualitative  
102 assessment of Q-Q plots [17]. Louie (2012) adopted a more comprehensive approach by first testing a  
103 number of standard copulas on wind speed data, and then eventually selecting Archimedean copulas [23].

104  
105 In modeling wind power, copulas have the highest utility in forecasting and in generating scenarios for  
106 optimization simulations [19]. These scenarios are necessary in stochastic programming, which is a critical  
107 decision tool in power systems analysis and planning research. For example, Gaussian copulas have been  
108 used to evaluate short-term scenarios for wind power generation [24], while empirical copulas have been  
109 used in modeling the dependency structure between the wind speed and the wind power output [25]. A  
110 quantile-copula kernel density estimator has also been used to improve probabilistic wind power forecasts  
111 [26].

112  
113 With respect to solar energy, temporal modeling of solar power generation has been done using  
114 generalized distribution functions that were subsequently optimized to ensure reliable and higher power  
115 outputs [27]. Solar irradiation is most often modeled using the Hollands and Huggets distribution, which  
116 can be approximated by the Gamma distribution [28]. To our knowledge, there has been no attempt to date

117 to model solar power generation using other types of probability distributions. Similar to wind power  
 118 generation, the dependence structure of solar systems is usually quantified by measures of association such  
 119 as linear correlation coefficients [29]. But in contrast to wind power generation, the spatial variability in  
 120 solar power generation in reasonably sized grids is not significant; thus modeling the spatial dependence of  
 121 solar power generated between dispersed locations is not necessary [30] but can be done with the method  
 122 we propose for wind power.

### 123 3. Methodology

124 Wind speed patterns and their spatial dependencies are generally non-Gaussian and non-linearly  
 125 correlated [14]. Since system planners are more interested in modeling wind power generation than wind  
 126 speeds, this presents a challenge because there is no standardization in modeling wind power using a  
 127 specific probability distribution. Therefore, in the present study, we use the Kumaraswamy distribution  
 128 for the temporal modeling of wind power generated at each site, and applied the concept of vine-copulas  
 129 to model wind power dependencies.

#### 130 3.1 Kumarawamy Distribution

131 First introduced in 1980, the double bounded Kumaraswamy distribution is a continuous probability  
 132 distribution that was originally developed for hydrology applications [26]. It is equivalent to the Beta  
 133 distribution but has a simpler analytical formulation, making it more efficient in computational  
 134 simulations. More importantly for this study, the Kumaraswamy distribution is selected because (i)  
 135 renewable power is a non-linear transformation of its resource (ex. wind power from wind speed) and (ii)  
 136 its simple analytical form allows for its easy integration with copulas.

137  
 138 The probability density function (PDF, ( $f(x)$ )) and cumulative density function (CDF, ( $F(x)$ ))  
 139 formulations of the Kumaraswamy distribution are given in Eq. 3.1 and Eq. 3.2, respectively, where  $a$  and  
 140  $b$  are shape parameters describing the distribution.

141

$$f(x) = abx^{a-1}(1-x^a)^{b-1} \quad (3.1)$$

142 Where,

$$a > 0, b > 0 \text{ and } x \in [0,1] \quad (3.2)$$

143

144 It has many of the same properties as the Beta distribution but has some advantages in terms of  
 145 tractability. The Kumaraswamy densities have similar behavior as the Beta densities such as they are  
 146 unimodal, uniantimodal, increasing, decreasing or constant depending on the parameters. Therefore, based  
 147 on the values of the shape parameters the densities take specific shape and exhibit certain properties such  
 148 as, if  $a > 1$  and  $b > 1$  then the density is unimodal, if  $a > 1$  and  $b \leq 1$  then the density is increasing,  $a < 1$  and  
 149  $b < 1$  then the density is uni-antimodal, and  $a \leq 1$  and  $b > 1$  then the density is decreasing. The densities are  
 150 log-concave if and only if the shape parameters are greater than or equal to 1.

151 In addition to hydrology, Kumaraswamy distribution is now widely used including in  
152 finance, statistical design centering of integrated systems, among others [31, 32].

### 153 3.2 Methodology

#### 154 3.2.1 Copulas and the Sklar Theorem

155 Copulas were first introduced in 1959 by the mathematician Abe Sklar [33] and have since become  
156 popular in describing the dependencies between random variables. Copulas are mathematical functions that  
157 allow us to combine univariate distributions to obtain a joint distribution with a particular dependence  
158 structure. The utility of a copula is most easily demonstrated in the use of distributions in probabilistic  
159 analysis. To illustrate, recall that the CDF of a distribution is used to draw a random variate. Most commonly,  
160 to draw a random value from a distribution, one starts by sampling from a uniform distribution,  $U(0,1)$ .  
161 This sample is treated as an observation of the variable's CDF; a sample can be drawn from the PDF by  
162 generating a uniform random number and transforming it using the CDF to a random value.

163  
164 Sklar's theorem is the theoretical foundation of copulas. It states that for a given joint multivariate  
165 distribution function and relevant marginal distributions for the corresponding random variables, there  
166 always exists a copula function that relates the marginal distributions of the variables. Mathematically, this  
167 can be derived as follows.

168  
169 Let  $F_{xy}$  be a joint distribution with margins  $F_x$  and  $F_y$ ; then there exists a copula  $C: [0,1]^2 \rightarrow [0,1]$  such  
170 that

$$f(x) = abx^{a-1}(1-x^a)^{b-1} \quad 3.3$$

171  
172 If the random variables,  $\mathbf{X}$  and  $\mathbf{Y}$  are continuous, then copula,  $C$  is unique; otherwise,  $C$  is uniquely  
173 determined on the (range of  $\mathbf{X}$ )  $\times$  (range of  $\mathbf{Y}$ ).

174  
175 Conversely if  $C$  is a copula and  $F_x$  and  $F_y$  are distribution functions, then the function  $F_{xy}$  is a joint  
176 distribution with margins  $F_x$  and  $F_y$ .

177  $C$  must be a function of particular type with certain properties as described by [33] and explained  
178 further in [19].

179  
180 The copula is further defined as follows.

181  $C$  is a copula if  $C: [0,1]^2 \rightarrow [0,1]$  and

$$182 \quad C(0, u_m) = C(v_m, 0) = 0$$

$$183 \quad C(1, u_m) = C(u_m, 1) = u_m$$

$$184 \quad C(u_{m2}, v_{m2}) - C(u_{m1}, v_{m2}) - C(u_{m2}, v_{m1}) + C(u_{m1}, v_{m1}) \geq 0 \text{ for all } v_{m1} < v_{m2}, u_{m1} < u_{m2}$$

185 If  $C$  is differentiable once in its first argument and once in its second then,  $C$  is equivalent to

$$186 \quad \int_{v_{m1}}^{v_{m2}} \int_{u_{m1}}^{u_{m2}} \frac{\partial^2 C}{\partial u_m \partial v_m} du_m dv_m \geq 0 \text{ for all } v_{m1} < v_{m2}, u_{m1} < u_{m2}$$

187 where  $u_m, v_m, u_{mi}, v_{mi}$  are marginal distribution functions.

188 This definition of a copula simply states that a copula is itself a distribution function, defined on  
189  $[0,1]^2$  with a uniform marginal. Each of the marginal distributions produces a probability of one-  
190 dimensional events. The copula function takes these probabilities and maps them to a joint probability,  
191 enforcing a relationship on the probabilities. Therefore, using copulas to build multivariate distributions is  
192 a very flexible and powerful technique as it separates choice of dependence from the choice of marginal  
193 [19].

194 Sklar's theorem establishes one of the easiest ways of constructing copulas. In this case, if  $F_x$  and  $F_y$   
195 are the marginal distributions, then a copula is given by the formulation in Eq. 3.4.

$$C(u_m, v_m) = F_{XY}(F_X^{-1}(u_m), F_Y^{-1}(v_m)) \quad 3.4$$

### 196 3.2.2 Selection of the Appropriate Copula

197 A critical step in modeling data using copulas is the selection of the appropriate copula function from  
198 among the family of copulas that best describes the given data set. The selection process is often based on  
199 the analytical tractability of the copula function [34]. Three types of copulas are considered in this study:  
200 Gumbel, Joe-Frank, and the Student t. The Gumbel copula is most suited for extreme distributions while  
201 the Joe-Frank and Student t copulas are more suited for applications with heavy dependence on tails [19,  
202 35].

203 The Gumbel copula is a bivariate Archimedean copula. It is an asymmetric copula that exhibits greater  
204 dependence on the positive tail than on the negative tail. This copula is given by Eq. 3.5, where  $\delta$  is the  
205 parameter controlling the dependence between the marginal distributions  $u$  and  $v$ .

$$C_\delta(u, v) = \exp(-[(-\log u)^\delta + (-\log v)^\delta]^{1/\delta}) \quad 3.5$$

206 The Joe-Frank copula, sometimes called the BB8 copula, is a two-parameter copula also from the  
207 Archimedean family of copulas. The copula CDF is given by Eq. 3.6, where the parameter  $\delta$  illustrates  
208 the degree of dependence between the marginal distributions  $u$  and  $v$ , and the parameter  $\vartheta$  is the degree  
209 of freedom.

$$C_{\vartheta, \delta}(u, v) = \delta^{-1} \left( 1 - \{1 - \eta^{-1}[1 - (1 - \delta u)^\vartheta][1 - (1 - \delta v)^\vartheta]\}^{1/\vartheta} \right) \quad 3.6$$

210 where

$$211 \quad \vartheta \geq 1 \text{ and } 0 \leq \delta \leq 1$$

$$212 \quad \eta = 1 - (1 - \delta)^\vartheta \text{ and } 0 \leq u, v \leq 1$$

213  
214 The Student t copula allows for joint fat tails and an increased probability of joint extreme events  
215 compared with the other copulas. Increasing the value of  $\vartheta$  decreases the tendency to exhibit extreme co-  
216 movements. The copula formulation is expressed in Eq. 3.7, where  $\rho$  and  $\vartheta$  are the parameters of the  
217 copula, and  $t_{\vartheta}^{-1}$  is the inverse of the standard univariate t-copula with  $\vartheta$  degrees of freedom, expectation  
218 0 and variance  $\frac{\vartheta}{\vartheta-2}$  [35]. The variables  $s$  and  $t$  are the random vectors obtained from the two marginal  
219 distributions.

$$C_{\rho, \vartheta}(u, v) = \int_{-\infty}^{t_{\vartheta}^{-1}(u)} \int_{-\infty}^{t_{\vartheta}^{-1}(v)} \frac{1}{2\pi(1-\rho^2)^{1/2}} \left\{ 1 + \frac{u^2 - 2\rho uv + v^2}{v(1-\rho^2)} \right\}^{-(\vartheta+2)/2} ds dt \quad 3.7$$

220

### 221 3.2.3 C-Vine Copulas

222 Joe [35] presented the first construction of a multivariate copula using (conditional) bivariate copulas,  
223 while Bedford and Cooke [36] developed a more general construction method of multivariate densities and  
224 introduced regular vines to organize different pair-copula constructions (PCCs). Vines are a graphical  
225 representation of constraints in high dimensional probability distributions. They are used to specify so-  
226 called PCCs, as introduced by Aas et al. [37].

227  
228 Conventionally, a copula model is limited to a 1-parameter or 2-parameter specification of the  
229 dependence structure, which represents a potentially severe empirical constraint. Clearly, when modeling  
230 the joint distribution of multiple variables, such limited parameter models are unlikely to adequately capture  
231 the dependence structure between variables. For example, the Gaussian copula lacks tail dependence.  
232 Similarly, while the multivariate Student t copula is able to generate different tail dependence for each pair  
233 of variables, it imposes the same upper and lower tail dependence across all pairs. These limitations are  
234 overcome by the canonical vine (C-vine) model by building bivariate copulas of conditional distributions.  
235 C-vine copulas are flexible multivariate copulas that are generated via hierarchical construction and can be  
236 decomposed into a cascade of bivariate copulas. The basic principle is to model dependence using simple  
237 local building blocks (pair-copulas).

## 238 4. Spatial and Temporal Modeling of Renewable Energy Resources

### 239 4.1 Algorithm for Temporal Modeling of Wind Power and for Scenario Generation

240 This section discusses the procedure for modeling wind power generation in various spatially  
241 dispersed sites using the generalized Kumaraswamy distribution and C-Vine copulas.

242  
243 Firstly, given temporal data sets (daily and seasonal) on the wind power generated at different  
244 installations, we use the Kumaraswamy model to describe the probability distribution of each data set. We  
245 obtain the model parameters for each hour of the day and for three seasons in the year lets call them Season  
246 1, Season 2, and Season 3 using the Maximum Likelihood Estimate (MLE) method for distribution fitting  
247 with historical data. This ensures that both hourly and seasonal variations are embodied in the distribution  
248 models. Therefore, we create for each hour of the day within each of the three seasons a distribution from  
249 all the measurements at that hour of day for all days within that season across a number of year. This leads  
250 us to create  $3 \text{ (season)} \times 24 \text{ (hours)} = 72$  distributions for each location. These distributions are then used  
251 to choose a C-Vine model for the installation site under consideration.

252  
253 In order to develop the C-Vine tree, one location must first be selected as the root node of the tree and  
254 the others its children (nodes). This is accomplished by generating the Kendall rank correlation matrix, and  
255 summing the correlations across each location with respect to the other locations. The location with the  
256 maximum value of the Kendall rank correlation is chosen as the root node.

257  
258  
259  
260  
261  
262  
263  
264  
265

Once the C-vine tree is constructed, various families of bivariate copulas are then fitted to model the dependence between the root node and each one of its children. We again use the MLE method to fit the copulas, and use AIC/BIC (Akaike Information Criterion/ Bayesian Information Criteria) to evaluate the goodness of fit. In this, pair-copula construction approach, a bivariate copula is fitted to the root node and the child. Finally, we utilize the PCC-based tree to produce scenarios by drawing data from the PCC followed by Kumaraswamy distribution for each hour of the day or season.

The algorithm for modeling of wind power is summarized in Table 1.

Step	Specific Action
1	Fit Kumaraswamy distribution to each location's hourly data for the three seasons (Season 1, Season 2 and Season 3) and obtain parameters for the distribution.
2	Compute the Kendall rank correlation matrix with correlation values where Correlation Values, location with respect to location
3	Formulate the Vine tree, where root is the location with $\max(\sum_{i,j} \sigma_{ij})$ .
4	Compute the Pair Copula Construction using the various copula options available
5	Generate scenarios from the PCC followed by inverse of Kumaraswamy CDF.

266  
267  
268

For scenario simulations using C-Vine, we generate the Vine matrix that defines the connections and parameter matrices containing the parameters of each of the copulas defined by each link.

269

#### 4.2 Algorithm for Spatial Modeling of Solar Power Generation

270  
271  
272  
273  
274  
275  
276  
277  
278  
279  
280  
281  
282  
283  
284

Similar to the procedure outlined in Section 4.1, we also use PCC for the spatial modeling of solar power generation. Our goal here is to develop a standardized approach for spatial modeling of renewable power sources. The procedure consists of two steps, as indicated in Table 2. Firstly, given the hourly (power generation) data at each location for the three seasons (Season 1, Season 2, and Season 3), we use the Kumaraswamy distribution to model hourly solar power outputs. We then generate scenarios by drawing random variables from the Kumaraswamy CDF for each day for the three seasons. Although, solar power is given by a strong deterministic component, and limiting the upper limit of the power output for each hour in the year, moderated by a stochastic process can be justified given the random behavior in solar insolation due to cloud cover, wind direction, smog, and other environmental factors.

Table 1. Steps in Modeling Solar Power Generation

Steps	Specific Action
-------	-----------------



Step 1	Fit Kumaraswamy distribution to each location's hourly data for the three seasons (Season 1, Season 2 and Season 3) and obtain parameters for the distribution.
Step 2	Generate scenarios from the Kumaraswamy CDF for each hour of day for the three seasons.

285

### 286 4.3 Model Optimization for the Optimal Allocation of Wind Turbines and Solar Panels

287 Once we obtain: (i) the model parameters for simulating data for a given site based on the marginal  
 288 distributions (i.e., Kumaraswamy distribution), and (ii) the dependence structure model parameters using  
 289 Vine-copulas, we can find an optimal allocation of wind power and solar power at each location in a given  
 290 space. For system planners, this information is important in deciding on the number of wind turbines and  
 291 solar panels that needs to be installed at each location to optimize power output.

292

293 In this study, our goal is to investigate the lower quantiles of the distribution of the overall renewable  
 294 energy (wind and solar) produced within a power system. These quantiles should be maximized to design  
 295 an optimal placement of the renewable energy installations. Because our approach is based on probability  
 296 distribution and the persistence in the hourly wind power is found to be not so strong in our data and we  
 297 can consider it to be independent for each hour. Similarly, for solar power since solar insolation follows a  
 298 daily pattern and the insolation at each hour can be considered independent. This allows us to model the  
 299 data using Kumaraswamy distribution and considered hourly variations as independent.

300

301 Suppose we have  $n$  locations in a given space (site). We need to make allocations of wind power and  
 302 solar panel installations at each location such that the allocation maximizes the overall power generation  
 303 and smoothens the total system power output. To reiterate, fluctuations in the total system output are due  
 304 to the erratic nature of the renewable sources as discussed in Sections 1 and 2. Thus, the overall objective  
 305 of the optimization problem is to minimize the negative effects of the erratic nature of the renewable energy  
 306 (wind and solar).

307

308 The optimization model is depicted in Eq. 3.8, where  $W_S$  and  $W_W$  are weightages of solar power and  
 309 wind power allocation at each location, respectively.  $X_{S,l}$  and  $X_{W,l}$  are solar and wind generation  
 310 scenarios, respectively, for each location  $l$  in the total  $n$  locations.

311

$$\max \text{Quantile}_\alpha(W_{W,S}^T X) \quad 3.8$$

312

$$\begin{aligned} & \text{where} \\ W_{W,S}^T X &= (W_{W_l} \times X_{W,l}) + (W_{S_l} \times X_{S,l}) \\ & l \in 1 \dots n, \text{ for all locations, s.t.} \\ & \sum_{i=1}^n W_{W_i} = 1 \\ & \sum_{i=1}^n W_{S_i} = 1 \end{aligned}$$

$$0 \leq W_{S_i}, W_{W_i} \leq 1$$

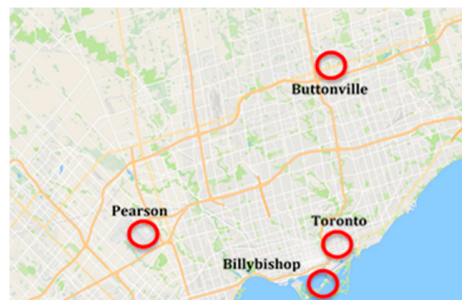
313

314 Eq. 3.8 represents the joint quantile optimization for solar and wind power allocation at a given site.  
 315 Such an approach tries to smoothen the power output in the entire power system by choosing an optimal  
 316 scheme for allocating solar and wind power resources. It also results in a more accurate modeling of the  
 317 renewable resources, as it considers not only the temporal but spatial features of wind power. Optimizing  
 318 the formulation in Eq. 3.8 will ensure that  $(1 - \alpha) * 100\%$  of all cases, the total power produced will be  
 319 above the  $\alpha$ -quantile.

## 320 5. Ontario Case Study

### 321 5.1 Location

322 The modeling methodology proposed in Section 4 has been applied in the case study of wind and solar  
 323 power systems in four sites in Central Ontario, Canada: Pearson, Toronto, BillyBishop, and Buttonville  
 324 (see Figure 1). These sites are important and unique due to their proximity to a densely-populated city (City  
 325 of Toronto) and a large water body (Lake Ontario), and their association with the main power grid in the  
 326 Greater Toronto Region. The power demand in this region is very high (27,000 MW /day on peak demand),  
 327 therefore it is critically important to achieve a stable power supply in the region. Increasing the penetration  
 328 of renewable energy-based systems, specifically wind power, may lead to instability in the available power  
 329 in the grid.



330

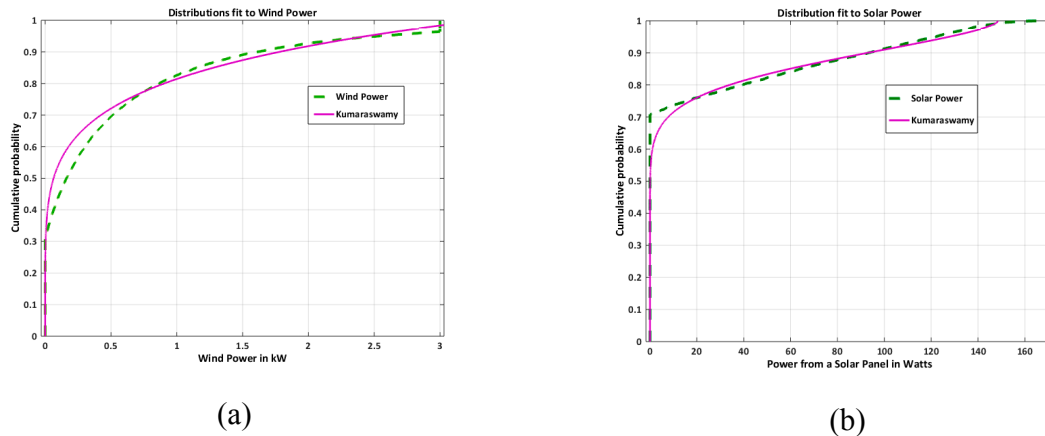
331

Figure 1: Central Ontario with all four locations under consideration

### 332 5.2 Fitting Probability Distribution Models to Wind and Solar Power Data

333 For the case study, we used data on solar power using the hourly solar insolation data for 3 years,  
 334 available through RETScreen [38]) and similarly data on wind power was generated using a wind turbine  
 335 [39] model for hourly wind speeds for 3 years for Toronto. Weibull is used as a standard for modeling wind  
 336 speed, log normal has been used at times as well and Gamma distribution has been sparingly used for  
 337 modelling solar insolation but there has been no standard distribution for fitting wind or solar power  
 338 generated. It is important as both wind speed and solar insolation undergo a non-linear transformation and  
 339 hence cannot be fit using either Weibull distribution for wind power or Gamma distribution for solar power.  
 340 Therefore, there is a need for a generalized distribution such as the Beta distribution that be used for fitting  
 341 both solar and wind power. We tested the Kumaraswamy distribution for fitting both solar power and wind  
 342 power data sets given its ability as a general distribution. It gives the flexibility and avoids the numerical

343 intractability that inhibit the use of the Beta distribution. The Kumaraswamy model best describes the  
 344 probability distribution of the data (see Figure 2) and hence will be used for the further study with copulas.



345 Figure 2: Probability distribution models fitted to data from Toronto, Ontario for Season 3 for the three year period  
 346 (a) Wind Power generated from Whisper 500 3kW wind turbine (b) to solar power from a 0.18kWp solar panel

### 347 5.3 Analysis of Wind Power for Dependence Modeling

348 We also performed a pair-wise comparison of wind power data (by transforming the wind speed  
 349 information obtained from RETScreen to power using the Whisper 500 wind turbine model at each of the  
 350 four sites. It is a Type 1 wind turbine.) for the four sites to determine the correlation between power data at  
 351 the sites (see Figure 3). Since the correlations appeared non-linear and data distribution was non-Gaussian,  
 352 we chose Kendall rank correlation as our correlation parameter. To ensure that the wind power data were  
 353 non-linearly correlated, we further grouped the data set for each paired site into 3 equal subsets. For each  
 354 site pairing, data were randomly assigned to a sub-group. An analysis of the data correlations in the subsets  
 355 independently revealed that the correlations varied markedly and were not constant for the sub-groups of  
 356 each paired site (see Figure 3). With the exception of one sub-group for the Toronto-Pearson paired location,  
 357 the Kendall rank values for all other sub-groups indicate non-linear behavior. For example, the sub-plot  
 358 between Buttonville and BillyBishop has an overall correlation of 0.26 whereas the corresponding three  
 359 subsets (low, medium, and high values) have varying correlation values of 0.06, 0.23 and 0.11.

### 360 5.4 C-Vine Copula Generation

361 Based on the observations of wind power behavior in Section 5.3, the wind power output at each  
 362 site are modeled using the Kumaraswamy distribution for each of the four sites in the case study to  
 363 generate pair-copula construction. We employed vine copulas to model the spatial dependence of wind  
 364 power production sites; this choice of copula was influenced by the following factors, as seen in Figure  
 365 3:

- 366 • the wind power in each location was non-normally distributed;
- 367 • the Kendall rank correlations of wind power between sites varied (the correlation coefficients  
 368 of the subplots of Figure 3 differ); and
- 369 • the wind power outputs at the sites were non-linearly dependent

370

371 The Kumaraswamy distribution was fitted to historical wind power data from each site. Maximum  
 372 likelihood estimates were used to obtain the distribution parameters. To model the dependence of  
 373 wind power generated from the four sites with C-vine copula, we first converted the wind power data  
 374 from the real domain to copula data, which lie inside the  $[0,1]$  hypercube. This was accomplished by  
 375 taking the Kumaraswamy CDF of the individual data series.

376

377 As described earlier in Section 4.1 (Step 3), we need to identify the root node of the C-Vine tree.  
 378 To do this, we generated the Kendall correlation matrix for the sites and added together the correlation  
 379 coefficients of each site (rightmost column of Table 3). This sum is an indicator of the strength of the  
 380 correlation of a site's wind power output to other locations' wind power outputs. Consequently, the  
 381 site with the highest the sum is selected as the root node of the C-vine tree. In our case study, the root  
 382 node of the C-vine tree is the Pearson site.

383

384

Table 2: Kendall Correlation Matrix for the Four Sites

385

Index		Toronto	Pearson	BillyBishop	ButtonVille	Sum
1	<b>Toronto</b>	1.000	0.811	0.561	0.213	2.585
2	<b>Pearson</b>	0.811	1.000	0.566	0.233	<b>2.610</b>
3	<b>BillyBishop</b>	0.561	0.566	1.000	0.255	2.382
4	<b>Buttonville</b>	0.213	0.233	0.255	1.000	1.701

386

387

388

389

390 The C-vine tree representation of our power generation sites is shown in Figure 5. The three other sites  
 391 (Toronto, BillyBishop and Buttonville) are connected to the root node (Pearson) by a link representing the  
 392 pair-copula construction between the root node and the site connected to it.

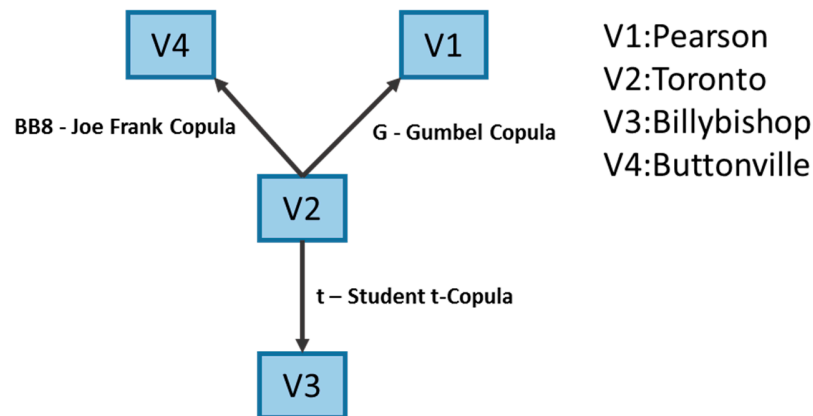
393

394 We used bivariate copulas to formulate the PCC for the three links. Each link represents a copula  
 395 describing the dependence in the marginal distributions of wind power at each site. We used the marginal  
 396 distribution (Kumaraswamy distribution) for each of the three site pairs and generated scenarios of power  
 397 production for each site. These generated data were then used to estimate the copula parameters. The choice  
 398 of the copula function was based on analytical tractability and simplicity and best fit to data. Copula fitting  
 399 was performed in R statistical software package (R version 3.2.4) using the CDVine package. We fitted the  
 400 data generated from the scenarios to a set of 24 copulas using maximum likelihood estimates and ranked  
 401 them based on the Akaike Information Criteria (AIC) and Bayesian Information Criteria (BIC).

402

403 For each link, the copulas with the largest AIC and BIC values were chosen for that particular link.  
 404 Figure 6 shows the results of the copula fitting. The Gumbel copula describes the dependence of the  
 405 marginal distributions of wind power between Pearson and Toronto, the Student-t copula describes the  
 406 Pearson-BillyBishop pair, and the Joe-Frank copula describes the Pearson-Buttonville pair.

407



408

409

Figure 3: Tree Estimated using Maximum Likelihood Estimates

410 Node labels represent the four sites in this case study: V1 (Pearson), V2 (Toronto), V3 (Billybishop)  
 411 and V4 (Buttonville) represent the four locations in our study. Link labels represent the copula chosen for  
 412 modeling the spatial dependence of wind power generation between the sites based on the maximum  
 413 likelihood estimates: BB8 (Joe-Frank), G (Gumbel) and t (Student-t).  
 414

### 415 5.5 Optimization of Power Allocation

416 Once the model of the probability distributions of renewable power is determined (wind, using  
 417 Kumaraswamy distribution and copulas; and solar, using Kumaraswamy distribution) the next step is to  
 418 find an optimal allocation (distribution of the total capacity of solar panels and wind turbines among sites)  
 419 of renewable energy technologies among the four sites (see Section 4.3). Table 4 shows the results of this  
 420 optimization. For solar power, the distribution of weights across the four sites tends to remain constant even  
 421 in cases where high reliability is desired ( $\alpha$  values range from 0.05 to 0.10). This implies low variations in  
 422 solar power generation across sites (i.e., stable power source). In contrast, for high reliability cases ( $\alpha$  values  
 423 range from 0.05 to 0.10), wind power distributions across the four sites exhibit more pronounced variations.  
 424 This implies that different power allocation strategies must be implemented to achieve higher and stable  
 425 power output from the 4 sites.

426

427

428

429

430

431

432

Table 3: Wind and Solar Allocation Weightages

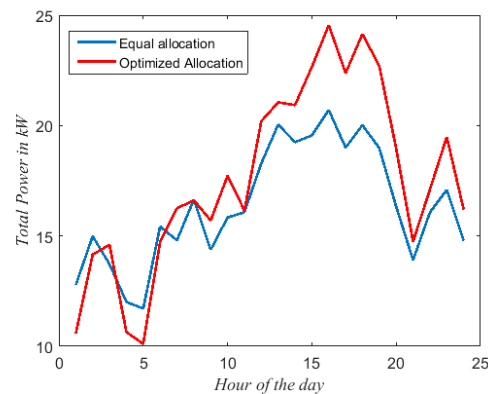
$\alpha$	$W_{W_1}$	$W_{W_2}$	$W_{W_3}$	$W_{W_4}$	$W_{S_1}$	$W_{S_2}$	$W_{S_3}$	$W_{S_4}$
----------	-----------	-----------	-----------	-----------	-----------	-----------	-----------	-----------

0.05	0.2556	0.2541	0.2619	0.2284	0.2498	0.2498	0.2505	0.2498
0.10	0.2670	0.2537	0.2381	0.2412	0.2500	0.2500	0.2500	0.2500
0.11	0.2486	0.2507	0.2492	0.2515	0.2500	0.2500	0.2500	0.2500
0.12	0.2499	0.2457	0.2587	0.2458	0.2500	0.2500	0.2500	0.2500
0.13	0.2529	0.2498	0.2538	0.2435	0.2485	0.2546	0.2485	0.2485
0.14	0.2609	0.2402	0.2588	0.2402	0.2486	0.2519	0.2508	0.2486
0.15	0.2551	0.2498	0.2484	0.2467	0.2496	0.2511	0.2496	0.2496

433

434  $\alpha$ :Reliability factor,  $W_{W_{1,2,3,4}}$ : Weightage of allocation for wind power technology at a site and  
 435  $W_{S_{1,2,3,4}}$ : Weightage of allocation for solar power technology at a site, where 1: Toronto, 2: Pearson,  
 436 3:Billybishop and 4: Buttonville

437 To illustrate the advantage of using this technique for allocating renewable energy technologies, we  
 438 compared the overall power generation (from wind and solar) when equal weightage across the four sites  
 439 is used, and when optimal allocation is used for  $\alpha = 0.05$ . A snapshot of power production for a 24-hour  
 440 period for the Season 3 months is shown in Figure 7. The optimized allocation technique results in  
 441 significantly higher and accurate overall power output during periods of peak power production.



442

443

Figure 7: Power production for various allocation schemes during the Season 3

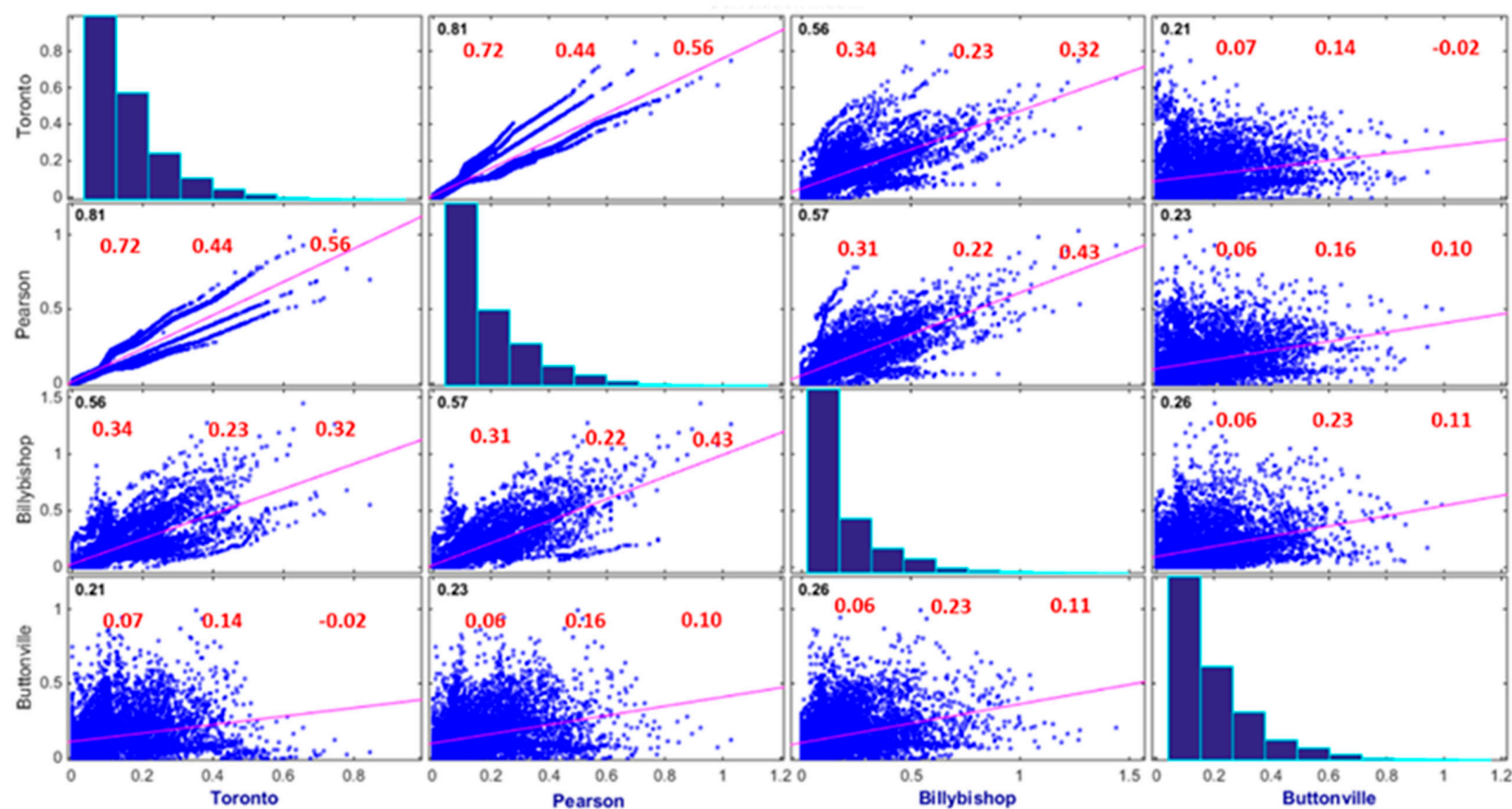


Figure 4: Pair-wise comparison of correlations in wind power data from 4 locations in Central Ontario. In the plots above the figures in black in each sub-plot represents the correlation coefficient for the entire data. Besides Pearson vs Toronto all other datasets are highly non-linear. Pink lines are least-square regression line whose slope is the correlation coefficient for the entire dataset. The panels in the main diagonal represent the histograms of the variables.

445

446 **6. Conclusions**

447 Copulas are one of the most sophisticated tools for modeling the dependence structure of  
448 between variables when their correlation is non-linear. In this paper, we present a methodology for  
449 modeling the non-linear spatial dependence in wind power generation using *copulas*. We modeled  
450 the temporal distributions of both wind and solar power for each individual location using the  
451 Kumaraswamy distribution. The data for solar and wind power generated from these probabilistic  
452 models is used in an optimization model for obtaining an appropriate allocation of solar and wind  
453 power technologies in a spatially dispersed landscape to maximize the overall power output and  
454 minimize the effect of random nature of the renewable sources of energy. We find that this approach  
455 is useful in increasing the overall reliability of energy production as well as accurate modeling of  
456 renewable resources.

457 **Acknowledgement**

458 This work was supported by the Natural Sciences and Engineering Research Council of Canada  
459 (NSERC). NSERC had no inputs in the study design, model development and implementation, and  
460 in the preparation of this manuscript.

461 **References**

- 462 1. D.E. Newton, World Energy Crisis: A Reference Handbook, ABC-CLIO, 2013 .
- 463 2. K. GILLINGHAM and J. SWEENEY, "BARRIERS TO IMPLEMENTING LOW-CARBON  
464 TECHNOLOGIES," *Climate Change Economics*, vol. 03, pp. 1250019, 2012.
- 465 3. F. Ribeiro, P. Salgado and J. Barreira, "Engineering Applications of Neural Networks: 13th International  
466 Conference, EANN 2012, London, UK, September 20-23, 2012. Proceedings," pp. 254-263, 2012.
- 467 4. D.L. King, W.E. Boyson and J.A. Kratochvil, "Analysis of factors influencing the annual energy production  
468 of photovoltaic systems," in *Photovoltaic Specialists Conference, 2002. Conference Record of the Twenty-  
469 Ninth IEEE*, pp. 1356-1361, 2002.
- 470 5. T. Hammons, "Integrating renewable energy sources into European grids," *International Journal of  
471 Electrical Power & Energy Systems*, vol. 30, pp. 462-475, 2008.
- 472 6. O. Grothe and J. Schnieders, "Spatial dependence in wind and optimal wind power allocation: A copula-  
473 based analysis," *Energy Policy*, vol. 39, pp. 4742-4754, sep. 2011.
- 474 7. B. Hasche, "General statistics of geographically dispersed wind power," *Wind Energy*, vol. 13, pp. 773-784,  
475 2010.
- 476 8. A. Gerber, M. Qadrdan, M. Chaudry, J. Ekanayake and N. Jenkins, "A 2020Â GB transmission network  
477 study using dispersed wind farm power output," *Renewable Energy*, vol. 37, pp. 124, 2012.
- 478 9. E. Kahn, "The reliability of distributed wind generators," *Electr.Power Syst.Res.*, vol. 2, pp. 1, 1979.
- 479 10. A. Abdollahi and M.P. Moghaddam, "Investigation of Economic and Environmental-Driven Demand  
480 Response Measures Incorporating UC," *IEEE Transactions on Smart Grids*, vol. 3, pp. 12-25, 2012.
- 481 11. D. D. Le, G. Gross and A. Berizzi, "Probabilistic Modeling of Multisite Wind Farm Production for Scenario-  
482 Based Applications," *IEEE Transactions on Sustainable Energy*, vol. 6, pp. 748-758, July. 2015.
- 483 12. K. Veeramachaneni, X. Ye and U. O'Reilly, "Statistical Approaches for Wind Resource Assessment,"  
484 *Computational Intelligent Data Analysis for Sustainable Development*, pp. 303, 2013.
- 485 13. D. P. Kroese, T. Taimre and Z.I. Botev, *Handbook of Monte Carlo Methods*, Wiley, 2013, .
- 486 14. J. S. Benth and F.E. Benth, "Analysis and modelling of wind speed in New York," *Journal of Applied  
487 Statistics*, vol. 37, pp. 893-909, 2010.
- 488 15. R. T. Clemen and T. Reilly, "Correlations and Copulas for Decision and Risk Analysis," *Management  
489 Science*, vol. 45, pp. 208-224, 1999.



- 490 16. H. Valizadeh Haghi, M. Tavakoli Bina, M.A. Golkar and S.M. Moghaddas-Tafreshi, "Using Copulas for  
491 analysis of large datasets in renewable distributed generation: PV and wind power integration in Iran,"  
492 *Renewable Energy*, vol. 35, pp. 1991-2000, 9. 2010.
- 493 17. S. Hagspiel, A. Papaemmanouil, M. Schmid and G. Andersson, "Copula-based modeling of stochastic wind  
494 power in Europe and implications for the Swiss power grid," *Appl. Energy*, vol. 96, pp. 33, 2012.
- 495 18. G. Papaefthymiou and D. Kurowicka, "Using Copulas for Modeling Stochastic Dependence in Power  
496 System Uncertainty Analysis," *Power Systems, IEEE Transactions On*, vol. 24, pp. 40-49, Feb. 2009.
- 497 19. R.B. Nelsen, *An introduction to copulas*, New York : Springer, c2006, 2006, .
- 498 20. P. Joubert, "Modelling Copulas : An Overview," pp. 1-27, .
- 499 21. Yih-Huei Wan, "Wind power plant behaviors: Analyses of long-term wind power data," NREL., Tech. Rep.  
500 NREL/TP-500-36551, 2004.
- 501 22. Bernhard Ernst, Yih-Huei Wan, Brendan Kirby, "Short-term power fluctuation of wind turbines: Analyzing  
502 data from the German 250-MW measurement program from the ancillary services viewpoint," NREL.,  
503 Tech. Rep. NREL/CP-500-26722, 1999.
- 504 23. H. Louie, "Evaluating Archimedean Copula models of wind speed for wind power modeling," in *Power  
505 Engineering Society Conference and Exposition in Africa (PowerAfrica)*, 2012 IEEE, pp. 1-5, 2012.
- 506 24. P. Pinson and R. Girard, "Evaluating the quality of scenarios of short-term wind power generation,"  
507 *Appl. Energy*, vol. 96, pp. 12, 2012.
- 508 25. S. Gill, B. Stephen and S. Galloway, "Wind Turbine Condition Assessment Through Power Curve Copula  
509 Modeling," *Sustainable Energy, IEEE Transactions On*, vol. 3, pp. 94-101, Jan. 2012.
- 510 26. R. J. Bessa, J. Mendes, V. Miranda, A. Botterud, J. Wang and Z. Zhou, "Quantile-copula density forecast for  
511 wind power uncertainty modeling," in *PowerTech*, 2011 IEEE Trondheim, pp. 1-8, 2011.
- 512 27. D. Heinemann, E. Lorenz and M. Girodo, "Forecasting of solar radiation," *Solar Energy Resource  
513 Management for Electricity Generation from Local Level to Global Scale*. Nova Science Publishers, New  
514 York, 2006.
- 515 28. G. Tina, S. Gagliano and V.A. Doria, "Probability Analysis of Weather Data for Energy Assessment of  
516 Hybrid Solar / Wind Power System University of Catania," in *4th IASME/WSEAS Interantional Conference  
517 on ENERGY, ECOSYSTEMS and SUSTAINABLE DEVELOPEMNT*, pp. 217-223, 2008.
- 518 29. A. Sfetsos, "A comparison of various forecasting techniques applied to mean hourly wind speed time  
519 series," *Renewable Energy*, vol. 21, pp. 23-35, 2000.
- 520 30. B. Tarroja, F. Mueller and S. Samuelson, "Solar power variability and spatial diversification: implications  
521 from an electric grid load balancing perspective," *Int.J. Energy Res.*, vol. 37, pp. 1002-1016, 2013.
- 522 31. A. Seifi, K. Ponnambalam and J. Vlach, "A unified approach to statistical design centering of integrated  
523 circuits with correlated parameters," *Circuits and Systems I: Fundamental Theory and Applications, IEEE  
524 Transactions On*, vol. 46, pp. 190-196, Jan. 1999.
- 525 32. A. Seifi, K. Ponnambalam and J. Vlach, "Optimization of filter designs with dependent and asymmetrically  
526 distributed parameters," *Journal of the Franklin Institute*, vol. 350, pp. 378, 2013.
- 527 33. A. Sklar, "Distribution functions of n dimensions and margins," *Publications of the Institute of Statistics of  
528 the University of Paris*, vol. 8, pp. 229-231, 1959.
- 529 34. W. Hurlimann, "Fitting bivariate cumulative returns with copulas," *Computational Statistics \& Data  
530 Analysis*, vol. 45, pp. 355-372, 2004.
- 531 35. H. Joe, *Multivariate Models and Multivariate Dependence Concepts*, Taylor \& Francis, 1997, .
- 532 36. T. Bedford and R. Cooke, *Probabilistic Risk Analysis: Foundations and Methods*, Cambridge University  
533 Press, 2001, .
- 534 37. K. Aas, C. Czado, A. Frigessi and H. Bakken, "Pair-copula constructions of multiple dependence,"  
535 *Insurance: Mathematics and Economics*, vol. 44, pp. 182-198, 2009.
- 536 38. G. J. Leng, A. Monarque, R. Alward, N. Meloche and A. Richard, "Canada's Renewable Energy Capacity  
537 Building Program & Retscreen International," in *Proceedings of the World Renewable Energy Congress  
538 VII*, Cologne, Germany, 2002.
- 539 39. Southwest Energy, "Specification Sheet Whisper 500,"  
540